

Importance of the donor:fullerene intermolecular arrangement for high-efficiency organic photovoltaics

Kenneth R. Graham, Clément Cabanetos, Justin P. Jahnke, Matthew N. Idso, Abdulrahman El Labban, Guy O. Ngongang Ndjawa, Thomas Heumueller, Koen Vandewal, Alberto Salleo, Bradley F. Chmelka, Aram Amassian, Pierre M. Beaujuge, and Michael D. McGehee

J. Am. Chem. Soc., **Just Accepted Manuscript** • Publication Date (Web): 16 Jun 2014

Downloaded from <http://pubs.acs.org> on June 24, 2014

Just Accepted

“Just Accepted” manuscripts have been peer-reviewed and accepted for publication. They are posted online prior to technical editing, formatting for publication and author proofing. The American Chemical Society provides “Just Accepted” as a free service to the research community to expedite the dissemination of scientific material as soon as possible after acceptance. “Just Accepted” manuscripts appear in full in PDF format accompanied by an HTML abstract. “Just Accepted” manuscripts have been fully peer reviewed, but should not be considered the official version of record. They are accessible to all readers and citable by the Digital Object Identifier (DOI®). “Just Accepted” is an optional service offered to authors. Therefore, the “Just Accepted” Web site may not include all articles that will be published in the journal. After a manuscript is technically edited and formatted, it will be removed from the “Just Accepted” Web site and published as an ASAP article. Note that technical editing may introduce minor changes to the manuscript text and/or graphics which could affect content, and all legal disclaimers and ethical guidelines that apply to the journal pertain. ACS cannot be held responsible for errors or consequences arising from the use of information contained in these “Just Accepted” manuscripts.



Importance of the donor:fullerene intermolecular arrangement for high-efficiency organic photovoltaics

Kenneth R. Graham,^{1,2} Clement Cabanetos,² Justin P. Jahnke,³ Matthew N. Idso,³ Abdulrahman El Labban,² Guy O. Ngongang Ndjawa,² Thomas Heumueller,¹ Koen Vandewal,¹ Alberto Salleo,¹ Bradley F. Chmelka,³ Aram Amassian,^{2***} Pierre M. Beaujuge,^{2**} Michael D. McGehee^{1*}

¹Department of Materials Science and Engineering, Stanford University, Stanford, CA 94305, United States.

²Division of Physical Sciences & Engineering, King Abdullah University of Science and Technology (KAUST), Thuwal 23955-6900, Saudi Arabia. ³Department of Chemical Engineering, University of California, Santa Barbara, Santa Barbara, CA 93106, United States

KEYWORDS: *Organic photovoltaic, organic solar cell, charge separation, organic-organic interface*

ABSTRACT: The performance of organic photovoltaic (OPV) material systems are hypothesized to depend strongly on the intermolecular arrangements at the donor:fullerene interfaces. A review of some of the most efficient polymers utilized in polymer:fullerene PV devices, combined with an analysis of reported polymer donor materials wherein the same conjugated backbone was used with varying alkyl substituents, supports this hypothesis. Specifically, the literature shows that higher-performing donor-acceptor type polymers generally have acceptor moieties that are sterically accessible for interactions with the fullerene derivative, whereas the corresponding donor moieties tend to have branched alkyl substituents that sterically limit interactions with the fullerene. To further explore the idea that the most beneficial polymer:fullerene arrangement involves the fullerene docking with the acceptor moiety, a family of benzo[1,2-b:4,5-b']dithiophene-thieno[3,4-c]pyrrole-4,6-dione polymers (PBDTTPD derivatives) was synthesized and tested in a variety of PV device types with vastly different aggregation states of the polymer. In agreement with our hypothesis, the PBDTTPD derivative with a more sterically accessible acceptor moiety and a more sterically hindered donor moiety shows the highest performance in bulk-heterojunction, bilayer, and low-polymer concentration PV devices where fullerene derivatives serve as the electron accepting materials. Furthermore, external quantum efficiency measurements of the charge-transfer state and solid-state two-dimensional (2D) ¹³C{¹H} heteronuclear correlation (HETCOR) NMR analyses support that a specific polymer:fullerene arrangement is present for the highest performing PBDTTPD derivative, in which the fullerene is in closer proximity to the acceptor moiety of the polymer. This work demonstrates that the polymer:fullerene arrangement and resulting intermolecular interactions may be key factors in determining the performance of OPV material systems.

INTRODUCTION

Organic photovoltaics (OPVs) are a promising PV technology due to their use of potentially low-cost and non-toxic materials, high performance in low light conditions, and their potential for solution processing on inexpensive flexible substrates.¹⁻³ Critical to the operation of an organic photovoltaic (OPV) device is the interface between an electron donating material and an electron accepting material, where photogenerated excitons are dissociated and separated into free charges. It is expected that the molecular arrangement at this interface and the resulting interfacial energetics play a major role in exciton dissociation, charge separation, and charge recombination processes,⁴ yet this important role remains to be clearly established.

Although hundreds, or even thousands, of OPV materials have been synthesized and studied,^{1,5-9} many questions still

remain as to what factors actually make a high performing OPV material. Some material properties that can lead to high performance are known, such as reasonably high charge-carrier mobility, broad and strong absorbance, and appropriate energy levels to form a type II heterojunction. However, many systems that display these properties yield only moderate or low performance,⁹⁻¹⁴ potentially because the intermolecular arrangements and resulting energy landscapes at the donor-acceptor interface are unfavorable for charge separation. The role that this interfacial arrangement can play is apparent in the theoretical literature, where calculated electron transfer rates,¹⁵ exciton binding energies,^{16,17} interfacial energetics,¹⁸⁻²¹ and charge separation probabilities^{16,22} vary dramatically based on the molecular arrangement between electron donating and electron accepting molecules. Any of these factors has the potential to greatly influence the performance of the OPV material system; however, probing the intermolecular arrangement is

experimentally difficult and thus its effects on device performance remain relatively untested.

The development of high-efficiency polymers and small molecules for PV applications has largely stemmed from the use of donor-acceptor (D-A) systems, whereby an electron-rich moiety (“donor”) is covalently bound to an electron-deficient (“acceptor”) moiety. In these D-A type systems the change in electron distribution between D and A moieties upon photoexcitation can vary substantially depending on the strength of the D and A moieties; though, in most D-A polymers utilized in OPVs the LUMO tends to be more localized on the A moiety, whereas the HOMO tends to be more delocalized over the D and A moieties.²³ These D-A compounds, generally either polymers or oligomers, are the electron donor materials in OPV devices and usually a fullerene derivative is the electron accepting material; thus, from here on “polymer” and “fullerene” will be used in reference to the electron donating and electron accepting materials, respectively, while donor and acceptor will be used in reference to the electron-rich and -deficient moieties of the electron donating material. Among other reasons, these D-A compounds are advantageous owing to the precise control over the optical gap and energy levels of the frontier molecular orbitals that can be achieved through varying the strength of the D and A moieties.^{6,24–26} Interestingly, a clear structural trend emerges in the alkyl substitution pattern for D-A compounds that show the highest performance in OPVs. That is, the donor moieties tend to have more bulky alkyl substituents while the acceptor moieties have less bulky or no alkyl substituents. Herein, by combining literature trends among OPV materials with a systematic study of a set of specifically designed polymers, we explore the hypothesis that the highest performing polymers have a chemical structure that en-

courages the fullerenes to dock with the polymer in a specific location. Generally, this specific location appears to be with the A moiety of the polymer, though in a few select literature examples the specific location may be with the D moiety.

RESULTS AND DISCUSSION

Many of the highest performing polymers reported in the literature are highlighted in Figure 1.^{27–40} The majority of these polymers have branched alkyl groups on the D moieties and either no or linear alkyl groups on the A moieties. This combination makes the A moieties more sterically accessible to the fullerene. For example, if a fullerene (essentially a ball of almost 1 nm diameter) is placed on top of each polymer backbone in Figure 1, the larger branched alkyl groups on the D moieties will sterically favor the fullerene to approach the A moieties. In **PTB7** and **PTDB2** there are branched alkyl groups on the A moieties, though these A moieties remain relatively accessible since the branch point is distanced from the conjugated backbone by a coplanar ester group.⁴¹ The phenyl groups in **PIDTT-DFBT** and **PIDTDTQx** are out of plane, thereby providing significant steric hindrance over the center of the D moiety.³³ Some exceptions of where the A moiety is more sterically hindered are polymers containing amide groups, such as **DPP**, **isindigo (II)**, and **BTI** (see **PDPPTPT**, **P(IIID-DTC)**, and **PBTI3T** in Figure 1, respectively). These exceptions may possibly be explained by a relatively strong interaction between amide groups and fullerenes that outweighs the steric hindrance arising from the branched alkyl groups. This strong amide-fullerene interaction has previously been observed in solution state studies of fullerenes in or with amide containing solvents.^{42,43}

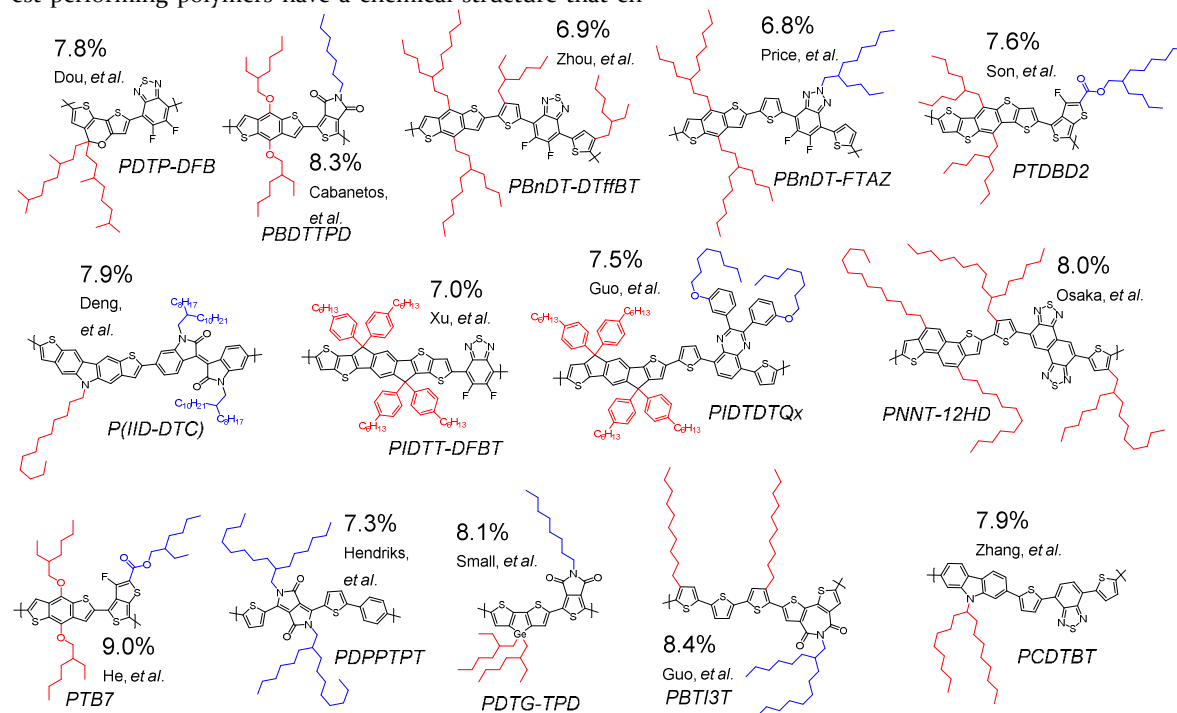


Figure 1. High performing PV polymers and their record power conversion efficiencies as reported in the literature, with red and blue substituents off the D and A moieties respectively.^{27–40}

A possible alternative explanation for the prevalence of certain alkyl substitution patterns in high-performing PV polymers is that these derivatives are more synthetically accessible. However, an analysis of the PV performance of multiple polymer families, where the alkyl groups are varied while the polymer backbone is kept constant, emphasizes the importance of the polymer-fullerene arrangement. In the majority of these polymers, the highest performance is achieved for polymers where the A moiety is more sterically accessible and the D moiety more sterically hindered. These materials are shown in Figure 2 and their PV performance characteristics listed in Table 1. The polymers are compared only among similar derivatives reported in the same publication or reported by the same research group, with lines in Table 1 separating the polymer families. Within each poly-

mer family, the polymer name is color-coded red, black, or green according to the performance trend that would be predicted based on the hypothesis that the highest performing material will result when the A moiety is more sterically accessible and/or the D moiety more sterically hindered. Red predicts a less sterically favorable polymer:fullerene arrangement with a more sterically accessible D moiety, black a more neutral arrangement with sterics not necessarily encouraging any particular arrangement, and green a favorable arrangement with the fullerene being encouraged to dock with the A moiety. The performance should thus increase from red to black to green, and as can be seen in Figure 2 and Table 1 the majority of polymers do follow the predicted trend.

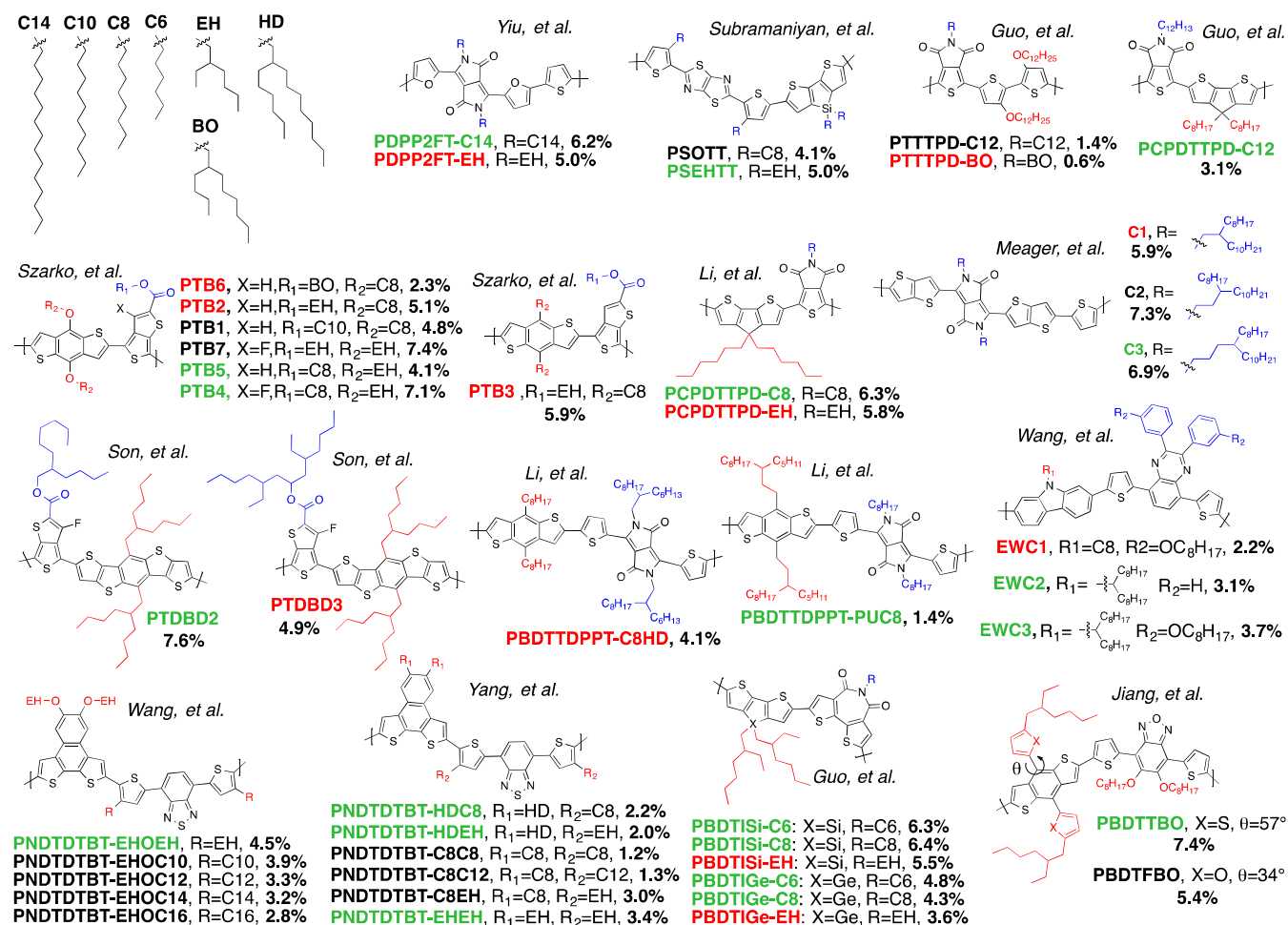


Figure 2. Donor polymers incorporated into polymer:fullerene bulk-heterojunction OPVs, wherein alkyl groups with varying bulkiness were utilized with the same conjugated backbone. Substituents are color coded in red or blue depending on whether they are off the D or A moiety, respectively. The color of the polymer acronym indicates the relative predicted performance in a polymer family based on the hypothesis described above. Note that some polymers are renamed from their original work, the renaming strategy is PXXXXYYY, where XXX is the donor moiety(s) acronym(s) and YYY is the acceptor moiety's acronym.

Table 1. Performance of organic photovoltaic cells for the polymers presented in Figure 2.

Polymer	J _{sc} (mA/cm ²)	V _{oc} (V)	FF	PCE	Follows predicted trend?
PDPP₂FT-C₁₄ ⁴⁴	14.8	0.65	0.64	6.2	Yes
PDPP₂FT-EH ⁴⁵	11.2	0.74	0.60	5.0	Yes
PSOTT ⁴⁶	10.2	0.62	0.65	4.1	Yes
PSEHTT	12.6	0.65	0.61	5.0	Yes
PTTTPD-C₁₂ ⁴⁷	7.36	0.41	0.48	1.44	Yes
PTTTPD-BO	1.59	0.59	0.54	0.57	Yes
PCPDTPD-C₁₂	8.12	0.76	0.50	3.06	Yes
PTB₆ ^{48,49}	7.74	0.62	0.47	2.26	Yes
PTB₂	12.8	0.60	0.66	5.10	No
PTB₃	13.9	0.72	0.59	5.85	No
PTB₁	12.5	0.58	0.65	4.76	No
PTB₅	10.7	0.66	0.58	4.1	No
PTB₇ ⁴⁸	14.5	0.74	0.69	7.4	Yes
PTB₄	15.5	0.70	0.65	7.1	Yes
PCPDTPD-C₈ ⁵⁰	14.1	0.75	0.61	6.31	Yes
PCPDTPD-EH	12.9	0.84	0.54	5.80	Yes
C₁ ⁵¹	16.6	0.59	0.60	5.9	Yes
C₂	18.6	0.61	0.64	7.3	Yes
C₃	18.7	0.60	0.62	6.9	Yes
PTDBD₂ ²⁸	13.0	0.89	0.653	7.6	Yes
PTDBD₃	10.7	0.88	0.521	4.9	Yes
PBDTTPPT-C₈HD ⁵²	9.4	0.71	0.61	4.1	No
PBDTTPPT-PUC₈	5.2	0.62	0.43	1.4	No
EWC₁ ⁵³	5.4	0.75	0.55	2.2	Yes
EWC₂	7.1	0.81	0.54	3.1	Yes
EWC₃	7.7	0.92	0.52	3.7	Yes
PNDTDTBT-EHOEH ¹⁴	10.5	0.70	0.61	4.5	Yes
PNDTDTBT-EHOC₁₀	9.36	0.68	0.63	3.9	Yes
PNDTDTBT-EHOC₁₂	7.85	0.68	0.58	3.3	Yes
PNDTDTBT-EHOC₁₄	7.35	0.73	0.59	3.2	Yes
PNDTDTBT-EHOC₁₆	6.64	0.67	0.63	2.8	Yes
PNDTDTBT-HDC₈ ⁵⁴	7.98	0.59	0.461	2.17	Yes
PNDTDTBT-HDEH	5.62	0.81	0.441	2.01	Yes
PNDTDTBT-C₈C₈	6.97	0.41	0.421	1.20	Yes
PNDTDTBT-C₈C₁₂	5.88	0.52	0.421	1.28	Yes
PNDTDTBT-C₈EH	10.93	0.59	0.464	3.00	Maybe
PNDTDTBT-EHEH	10.67	0.69	0.459	3.36	Yes

PBDTISI-C6 ⁵⁵	12.59	0.825	0.606	6.29	Yes
PBDTISI-C8	12.81	0.803	0.623	6.41	Yes
PBDTISI-EH	12.50	0.834	0.531	5.54	Yes
PBDTIGe-C6 ⁵⁵	12.30	0.774	0.502	4.77	Yes
PBDTIGe-C8	12.17	0.745	0.472	4.32	Yes
PBDTIGe-EH	10.09	0.769	0.467	3.62	Yes
PBDTTBO ⁵⁶	12.8	0.86	0.67	7.4	Yes
PBDTFBO	11.2	0.81	0.60	5.4	Yes

All the polymers displayed in Figure 2 have been incorporated into bulk-heterojunction (BHJ) devices, with either PC₆₁BM or PC₇₁BM as the fullerene derivative. Considering these are all BHJ devices and the nanoscale morphology will significantly influence device performance, it is even more remarkable that the majority of the reported polymers follow the predicted trend. The two notable exceptions are the DPP containing PBDTTPD derivatives and some of the PTB derivatives. The reason these materials do not follow the predicted trend may be due to nanoscale morphology differences, differences in fullerene solubility in the mixed phase,⁵⁷ a sufficiently sterically accessible acceptor moiety in all derivatives, and/or favorable intermolecular interactions between the A moieties and the fullerene that lead to a preferred arrangement regardless of alkyl substitution pattern. The PNDTDTBT-C8EH derivative is listed as “maybe” in the table due to the bulky EH groups on the thiophenes pointing towards the central NDT donor moiety, and thereby providing some steric bulk around that moiety as well as the thiophenes. An alternative explanation regarding the role of a specific polymer:fullerene arrangement, which may not necessarily be fullerene docking with the A moiety, will be presented later in the manuscript and would encompass some of the aforementioned exceptions. Importantly, some of the polymers listed in Figure 2 and Table 1 that have a favorable alkyl substitution pattern still only have PCEs in the 3-4% range. These moderate PCEs highlight that an appropriate alkyl substitution pattern does not guarantee a high PCE, as several other properties, such as absorbance, blend film morphology, and charge-carrier mobilities, must also be optimized for a high performing OPV material system.

In this work the family of PBDTTPD derivatives shown in Figure 3b are compared,⁵⁸⁻⁶⁰ whereby the alkyl groups appended to the donor and acceptor moieties are either linear or branched. Varying the alkyl groups between linear C₈H₁₇ (C8) or C₁₄H₂₉ (C14) and branched 2-ethylhexyl (EH) groups alters steric accessibility to the D and A units. As shown schematically in Figure 3a, the branched alkyl group is expected to provide steric hindrance and direct the fullerene to be closer to the linearly substituted unit. According to our hypothesis the highest performing derivative will have the branched EH group on BDT and the linear C8 group on TPD, referred to as EH/C8. The nomenclature used throughout this manuscript indicates the alkyl substituents on the BDT moiety followed by the substituent on the TPD moiety, i.e. C14/C8 is the derivative where R₁=C14 and R₂=C8.

The materials were all synthesized in a similar manner to yield polymers with comparable impurities and end groups. Number average molecular weights (M_n) are similar at 38, 38, and 36 kDa for the C14/C14, C14/C8, and EH/C8 derivatives, respectively, and slightly lower at 21 and 19 kDa for the C14/EH and EH/EH derivatives, respectively. All polymers have similar PDIs of 1.7 to 2.0. The lower M_n of derivatives with EH on the TPD unit may result in some performance variations,⁶¹ though the M_n alone is unlikely to explain the device results for the variety of device architectures presented herein. As shown in Supporting Information Figure S1, thin films of all the PBDTTPD derivatives show similar absorbance spectra with nearly identical optical gaps. These similarities in absorbance spectra suggest that varying the alkyl substitution pattern does not significantly affect electronic structure, molecular planarity, and conjugation length.

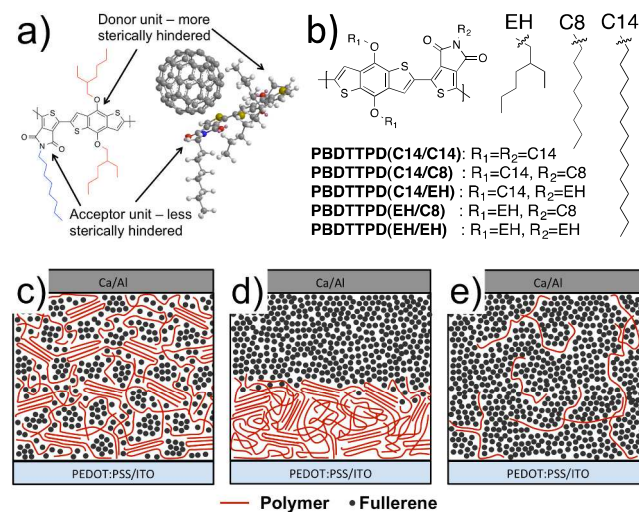


Figure 3. a) Proposed model illustrating how branched alkyl groups on the donor unit direct the fullerene towards the acceptor unit in PBDTTPD(EH/C8), b) the PBDTTPD family of polymer derivatives designed to sterically favor different polymer:fullerene arrangements, and schematics of the c) 3-phase BHJ morphology,^{57,62,63} d) bilayer, and e) low polymer content device architectures.

To experimentally test whether the OPV performance is in part determined by the molecular arrangement at the polymer:fullerene interface, the series of OPV device types presented in Figure 3c-e are examined. These include standard BHJ architectures with PC₆₁BM as the electron accepting

material, bilayer OPV devices with C₆₀ as the electron accepting material, and low polymer concentration devices whereby 1 to 8 wt.% of polymer is blended in a PC₆₁BM matrix. The bilayer and low-polymer concentration devices are included to reduce nanoscale morphology effects and minimize the influence of polymer-polymer interactions. In all device types the **EH/C8** derivative, where the branched substituent is on the BDT (donor) moiety and the linear substituent is on the TPD (acceptor) moiety, outperforms the other derivatives in terms of J_{SC} and overall PCE.

BHJ devices of the polymer:fullerene blends were all optimized for film thickness, polymer:fullerene ratio, and solvent additives for each individual polymer. All polymers showed similar optimized conditions, and therefore results are presented with identical fabrication conditions. As evident in Table 2 and the J-V curves included in the Supporting Information, the **EH/C8** derivative outperforms the other materials in BHJ devices, with a 40 to 170% higher J_{SC} and a 1 to 38% higher FF vs. the other derivatives. As a result the PCE is 6.0% for the **EH/C8** derivative as compared to 3.8% for the next highest performing derivative. The PCE of 6.0% for the **EH/C8** derivative is lower than can be achieved with PC₇₁BM and comparable to the previous value reported with PC₆₁BM and no solvent additives of 6.3%.⁵⁹ The higher performance for the **EH/C8** derivative is in agreement with the proposed model, though it is difficult to make any definitive conclusions from these trends given the large number of variables contributing to the performance of a BHJ device. For example, the performance of a BHJ device depends strongly on the

details of the nanoscale morphology, including the domain sizes and fullerene solubility in the mixed phase,^{57,64,65} and these differences are nearly impossible to distinguish from other factors such as polymer:fullerene intermolecular arrangements. Bilayer device architectures, as shown in Figure 3d, were thus fabricated and tested to eliminate the effects of nanoscale morphology differences.

The results of bilayer (BL) OPV devices with a pure polymer layer and a thermally evaporated pure C₆₀ layer are presented in Table 2 and Supporting Information Figure S3. To minimize interfacial mixing between C₆₀ and the polymers, the substrates were cooled down to ca. 0 °C during C₆₀ deposition. Similar to the BHJ results, the **EH/C8** derivative outperforms the other derivatives with a PCE of 1.5% vs. 1.1% for the next most efficient **EH/EH** derivative. The trends in these BL devices are relatively comparable to the trends in the BHJ devices with a few exceptions. The main exception is that the **C14/EH** derivative shows a comparable PCE to the linearly substituted **C14/C14** and **C14/C8** derivatives, whereby in the BHJ devices the J_{SC} and PCE of the **C14/EH** based OPV device is only half that of the **C14/C14** based device. This discrepancy between BHJ and BL device trends is most likely due to nanoscale morphology differences in the BHJ devices. The V_{OC} values for the BL devices are 0.07 to 0.10 V lower than the BHJ devices, which is likely the result of replacing PC₆₁BM with with the more electronegative C₆₀, as demonstrated previously for bilayer cells.⁶⁶

Table 2. Performance of organic photovoltaic cells based on BHJ and BL architectures with standard deviations indicated.

Material	Architecture	J _{SC} (mA/cm ²)	V _{OC} (V)	FF	PCE (%)
C14/C14	BHJ	6.3±0.1	0.94±0.01	0.65±0.07	3.8±0.1
C14/C8	BHJ	6.9±0.3	0.90±0.02	0.53±0.02	3.3±0.2
C14/EH	BHJ	3.6±0.2	0.97±0.01	0.48±0.03	1.7±0.2
EH/C8	BHJ	9.6±0.2	0.94±0.01	0.66±0.01	6.0±0.3
EH/EH	BHJ	6.6±0.4	0.96±0.03	0.50±0.03	3.2±0.3
C14/C14	BL	1.3±0.1	0.84±0.02	0.63±0.02	0.70±0.03
C14/C8	BL	1.2±0.1	0.80±0.01	0.66±0.01	0.63±0.02
C14/EH	BL	1.5±0.3	0.85±0.01	0.58±0.05	0.70±0.08
EH/C8	BL	2.7±0.3	0.87±0.01	0.66±0.01	1.5±0.1
EH/EH	BL	2.1±0.1	0.89±0.03	0.58±0.02	1.1±0.1

To decrease the effects of polymer-polymer interactions present in the BHJ and bilayer devices, low polymer concentration devices with 1 to 8 wt.% polymer in PC₆₁BM were fabricated and characterized.⁶⁷ As shown schematically in Figure 3e, it is expected that predominantly isolated polymer strands are present as opposed to polymer aggregates. With the polymer backbones all being identical, and presumably minimal polymer-polymer interchain interactions, the differ-

ences in performance should be primarily related to how the polymers interact with the fullerene.

In these low polymer concentration devices the best performing polymer is again the **EH/C8** derivative. This derivative shows approximately twice the J_{SC} and PCE as the other derivatives in the 1,2,4, and 8% polymer devices as shown in Figure 4 and the J-V curves in the Supporting Information. The relatively large standard deviations across multiple de-

1 vice sets may be attributed to variations in PC₆₁BM batch and
 2 uncertainties associated with the low polymer concentra-
 3 tions ($\pm 15\%$). To probe whether or not differences in device
 4 performance can be attributed to a difference in the number
 5 of excitons reaching a polymer-fullerene interface, photolu-
 6 minescence spectra of the blend films were measured. At a
 7 polymer concentration of 2% the fullerene emission is $34 \pm$
 8 5% quenched for the C₁₄/EH, EH/C8, and EH/EH blends
 9 and $26 \pm 5\%$ quenched in the C₁₄/C₁₄ and C₁₄/C8 blends, as
 10 shown in Supporting Information Figure S6. This similar
 11 quenching behavior indicates performance differences are
 12 not likely due to an increased number of excitons reaching a
 13 polymer:fullerene interface. With similar exciton quenching
 14 behavior it is also likely that at this low polymer concentra-
 15 tion there are not significant differences in the amount of
 16 polymer aggregation, which is expected to be minimal. At
 17 higher polymer concentrations of 4 and 8% some aggrega-
 18 tion does occur as observed through transmission electron
 19 microscopy (TEM) and grazing incident wide angle X-ray
 20 scattering (GIWAXS), see Supporting Information, though
 21 this does not change the trend in device performance.

22 To determine whether the performance differences were in
 23 part due to differences in non-geminate charge recombi-
 24 nation dynamics, the charge-carrier lifetimes for non-
 25 geminate recombination were measured by transient photo-
 26 voltage (TPV) as described by Shuttle, *et al.*⁶⁸ These TPV
 27 measurements were performed on PV devices with 2% poly-
 28 mer:98% PC₆₁BM, Supporting Information Figure S5, as in
 29 these devices polymer aggregation is minimized as compared
 30 to the 4 and 8% polymer devices. At one sun light intensity
 31 all polymers show a very similar lifetime of *ca.* 3 μ s, with
 32 no correlation between short circuit current and charge carrier
 33 lifetime. Furthermore, as a function of carrier density the
 34 charge-carrier lifetime τ is almost identical for EH/C8 and
 35 EH/EH. These similar bimolecular recombination lifetimes
 36 indicate that differences in PV performance cannot be
 37 explained by differences in non-geminate recombination rates,
 38 thus leaving differences in geminate recombination as the
 39 most likely factor in differentiating the PV performance.
 40 With the same conjugated backbone, similar emission
 41 quenching behavior, similar bimolecular recombination dy-
 42 namics, and predominantly polymer:fullerene interactions
 43 present, the most straightforward explanation for the differ-
 44 ences in device performance is that the probability of charge
 45 separation or geminate recombination is dependent on the
 46 interfacial polymer:fullerene arrangement. Therefore, these
 47 results support the hypothesis that the highest performance
 48 of the EH/C8 derivative originates from favorable docking of
 49 the fullerene with the A moiety of the polymer.

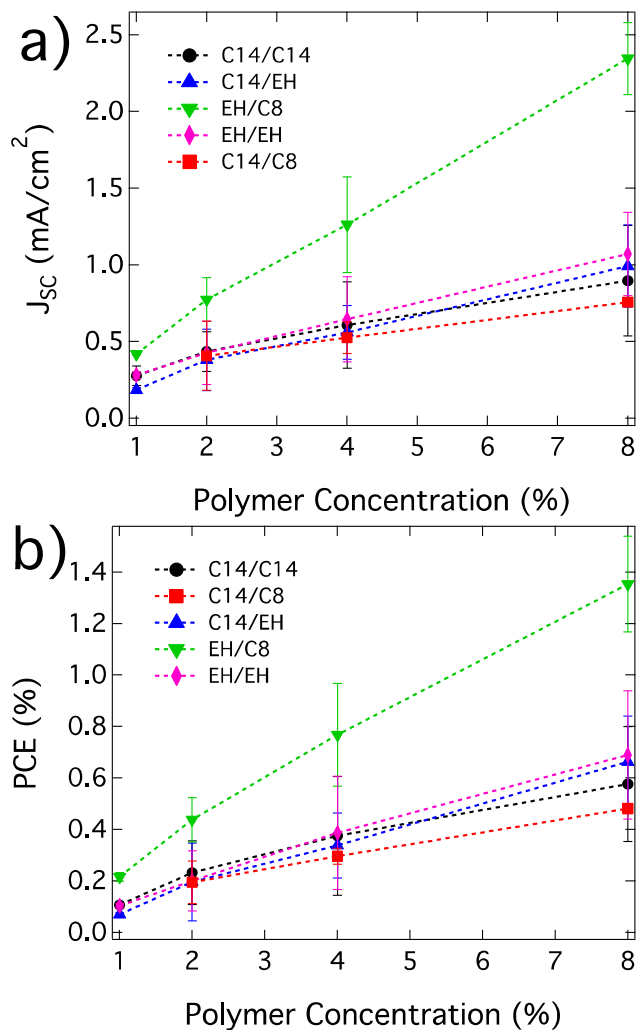


Figure 4. J_{SC} (a) and PCE (b) of polymer:PC₆₁BM solar cells where the concentration of polymer was varied from 1 to 8% by weight relative to the total solids concentration. Error bars represent standard deviations of several device sets made with varying batches of PC₆₁BM.

One method of directly probing the polymer:fullerene interfacial energetics is through the charge-transfer (CT) state absorbance, where the CT state is an intermolecular state formed between the polymer and fullerene.⁶⁹ This CT state can be probed with sensitive absorbance or EQE measurements, as shown in Figure 5. With interfacial energetics determined in part by intermolecular interactions, e.g. dipolar and quadrupolar,¹⁹ the CT state absorbance is sensitive to the molecular arrangement at the polymer:fullerene interface. Figure 5 shows the CT region of the EQE spectra and fits to the CT band for the devices with polymer concentrations of 2 and 4%, where the data is fit with equation 1:^{69,70}

$$EQE \propto \frac{f}{E\sqrt{4\pi\lambda kT}} \exp\left(\frac{-(E_{CT} + \lambda - E)^2}{4\lambda kT}\right) \quad (1)$$

Here, k is the Boltzmann constant, f is a term that accounts for the internal quantum efficiency, number of CT states, and electronic coupling, E_{CT} is an effective energy of the CT state and λ is related to the width of the CT absorbance band. More specifically, λ contains a reorganization energy term

(λ_0) that applies to a particular CT state environment and an energetic disorder term that reflects heterogeneities in CT state molecular arrangement and environment resulting from the restrictive, inhomogeneous solid-state film. λ_0 is the difference in energy between a vertically excited CT state with the same nuclear coordinates as the lowest energy ground CT state and the energy minimum of the excited CT state after environmental (low frequency) and internal (high frequency) reorganization,^{69,71,72} where in traditional liquid systems the environmental term is due to solvent reorganization. In the solid state, where inhomogeneous environments exist and nuclear positions are more constrained, the intermolecular arrangement and environment around each unique CT pair can give rise to significant differences in absorbance and emission characteristics.^{73,74} In a film consisting of many unique CT state environments these differences lead to greater optical peak widths and thereby increases in λ . Thus, in the polymer:PC₆BM films analyzed here λ results from internal reorganization, environmental reorganization, and energetic disorder components. With the energy of a CT state depending on the molecular arrangement,^{77,75} energetic disorder and λ will be reduced if a more specific molecular arrangement exists. From the fits of the data shown in Figure 5, we indeed find large differences in λ . For example, λ for the 4% **EH/C8**:PC₆BM blend is 0.08 eV vs. 0.21 eV for the 4% **EH/EH**:PC₆BM blend

To confirm that energetic disorder contributes to λ , we investigate a system with a known low amount of disorder and a well-defined and specific polymer:fullerene arrangement, i.e. the PBTTT:PC₇BM bimolecular crystal.⁷⁶ Analysis of the CT region of EQE spectra for the PBTTT:PC₇BM bimolecular crystal shows one of the narrowest CT absorbance bands of all BHJ systems, with λ of 0.12-0.13 eV (Supporting Information) compared to 0.2-0.4 eV for other BHJ systems.^{69,77,78} This narrow CT absorbance band is indeed consistent with a more specific polymer-fullerene conformation.

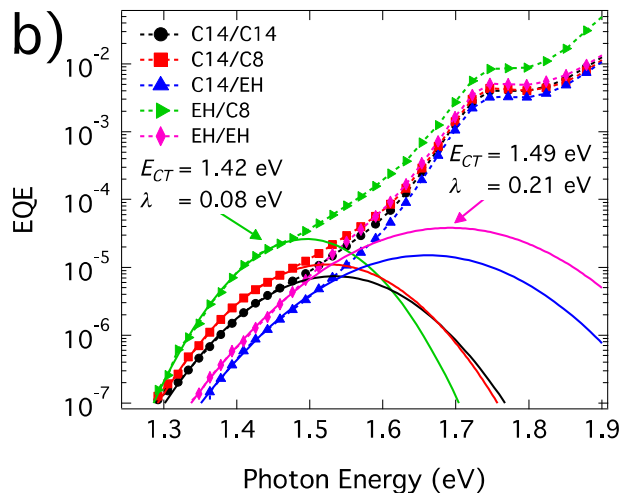
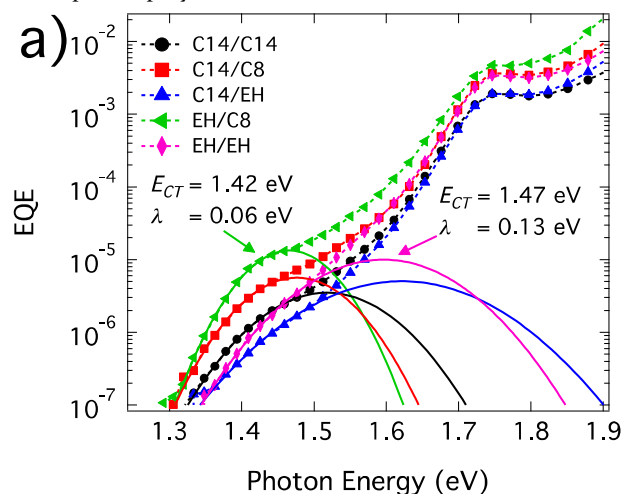


Figure 5. EQE spectra of the CT region, with fits to equation 1 indicated with solid lines, for polymer concentrations of a) 2 and b) 4%.

As evident from Figure 5 and the Supporting Information, **EH/C8** in PC₆BM shows the narrowest CT bands with λ of 0.06 and 0.08 eV for the 2 and 4% devices, respectively. This narrower CT band for the **EH/C8** derivative is in agreement with a more specific and consistent arrangement between polymer and fullerene, as a broader distribution of polymer:fullerene arrangements would increase the energetic distribution of CT states and increase λ . Displaying a slightly higher λ of 0.10 eV for the 2% polymer concentration device is the **C14/C14** derivative. When a branched chain is present on the TPD unit in **EH/EH**, λ is even higher at 0.13 eV for the 2% blend. A potential reason for this trend is that the EH group on TPD limits the otherwise energetically favorable TPD interaction with the fullerene, thus leading to a broader distribution of polymer:fullerene intermolecular arrangements. Another potential explanation for the decreased λ with the linear substituted TPD derivatives is that the fullerene is closer to the polymer backbone, as smaller center-center distances between molecules in a CT complex will reduce the environmental reorganization term.⁷¹ When the polymer concentration is increased to 8% the CT bands are broader for all polymers, with λ values of 0.2 to 0.3 eV. This broadening of the CT band most likely results from polymer aggregation occurring at these higher concentrations, where the aggregate regions of varying order would result in a wide spread of energy states. The narrower band at low concentration is another indicator that the majority of the polymers are more dispersed and minimally aggregated at low concentrations. The fact that all device types show the highest performance for the **EH/C8** derivative, regardless of the degree of polymer aggregation, is in agreement with the hypothesis that a specific polymer:fullerene arrangement leads to improved charge separation.

Solid-state nuclear magnetic resonance (NMR) spectroscopy complements the EQE measurements of the CT states by providing molecular-level insights on the interactions of the fullerene with the donor and acceptor moieties in the conjugated polymers. Specifically, solid-state two-dimensional (2D) ¹³C{¹H} heteronuclear correlation

(HETCOR) NMR measurements exploit through-space dipole-dipole couplings of locally proximate (< 1 nm) ^{13}C and ^1H nuclei to correlate their isotropic chemical shifts. This provides direct information on intra- and key intermolecular interactions among the chemically distinct polymer and fullerene moieties shown in Figure 6a and b, which depicts the PC₆₁BM functional groups (orange), the linear alkyl chains (blue), the branched EH alkyl groups (red), and the polymer backbone (brown). In particular, the 2D $^{13}\text{C}\{^1\text{H}\}$ HETCOR spectra of the neat EH/C8 and C14/EH conjugated polymers and PC₆₁BM (Supporting Information) yield well-resolved ^1H and ^{13}C signals that are confidently assigned to the specific polymer and PC₆₁BM moieties, labeled in Figure 6a, as indicated above the respective 1D ^1H and ^{13}C MAS spectra in Figure 6c.

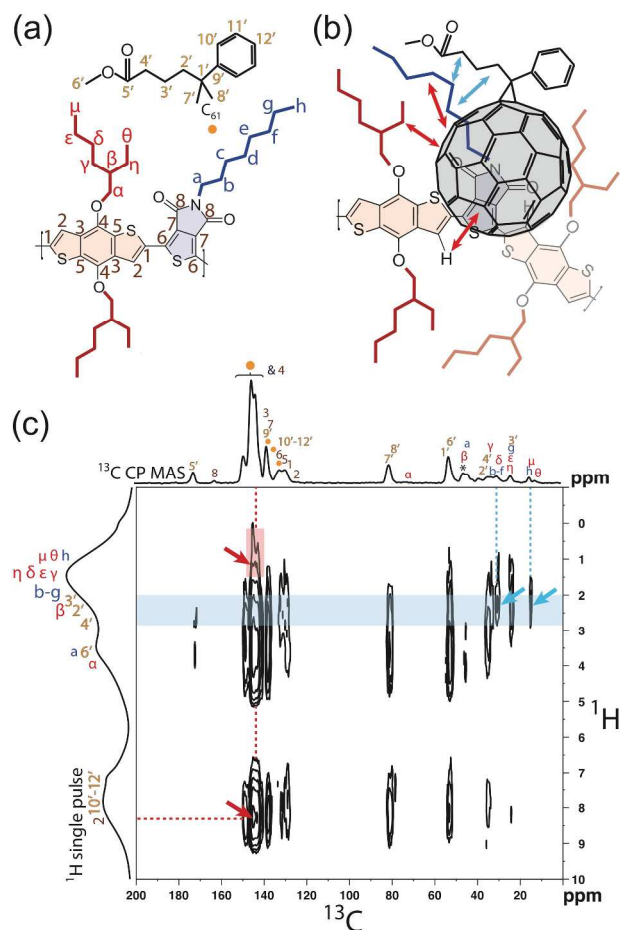


Figure 6. Molecular structures of (a) EH/C8 and PC₆₁BM, with their respective moieties labeled and (b) schematic showing red and blue arrows that indicate intermolecular interactions between the conjugated polymer and PC₆₁BM moieties that are consistent with the 2D NMR intensity correlations. (c) Solid-state 2D $^{13}\text{C}\{^1\text{H}\}$ dipolar-mediated heteronuclear correlation (HETCOR) NMR spectrum acquired at room temperature for an 8 wt% EH/C8 in PC₆₁BM blend under MAS conditions of 12.5 kHz, with an 8-ms CP contact time. 1D $^{13}\text{C}\{^1\text{H}\}$ CPMAS and single-pulse ^1H MAS spectra are shown along the top horizontal axis and the left vertical axis, respectively.

To gain insight into the polymer-fullerene intermolecular arrangement, 8 wt. % polymer, 92% PC₆₁BM blends were probed with 2D $^{13}\text{C}\{^1\text{H}\}$ HETCOR NMR. Although some aggregation is evident at 8 wt. % polymer, these higher polymer concentrations are necessary to maximize the 2D $^{13}\text{C}\{^1\text{H}\}$ HETCOR signal arising from polymer-fullerene interactions. For the 8 wt.% EH/C8 in PC₆₁BM blend, the 2D $^{13}\text{C}\{^1\text{H}\}$ HETCOR spectrum acquired at room temperature also yields well-resolved correlated signals, most of which reflect the same intramolecular contributions as for the neat components. Importantly, however, additional 2D intensity correlations are observed in Figure 6c that directly establish intermolecular interactions between the PC₆₁BM and EH/C8 polymer moieties. Specifically, ^{13}C signals associated with the C₆₀ fullerene group at 140-148 ppm are strongly correlated with the ^1H signals at *ca.* 1.2 ppm and *ca.* 8.3 ppm (Figure 6c, red arrows) associated with the alkyl and aromatic ^1H moieties of the polymer, respectively. It is noteworthy that the only ^1H atoms on the polymer backbone are associated with carbon site 2 of the BDT unit, each of which is adjacent to a TPD moiety. Similar correlated intensities are observed in the 2D $^{13}\text{C}\{^1\text{H}\}$ spectrum (Supporting information, Figure S9) of the 8 wt.% C14/EH in PC₆₁BM blend. These 2D intensity correlations unambiguously establish the close (< 1 nm) proximities of the C₆₀ moieties of the PC₆₁BM molecules to the polymer backbone for both of the EH/C8 and C14/EH heterojunction blends, as required for efficient charge transfer.

The 2D NMR results furthermore suggest that the type and placement of the alkyl groups influence the local configurations of the PC₆₁BM moieties near the polymer backbone. In particular, the ^{13}C signals at 31 ppm and 14 ppm that are associated with carbon atoms *b-f* and *h*, respectively, of the linear C8 alkyl chains on the TPD acceptor moiety are strongly correlated (Figure 6c, blue arrows) with the ^1H signals at 2-3 ppm from moieties 2'-4' of the PC₆₁BM functional group (Figure 6c, blue band). While the ^{13}C signal at 31 ppm contains overlapping signals from carbon atoms *b-f* of the linear C8 alkyl chain and δ of the branched EH alkyl groups, most of this signal intensity appears to arise from the ^{13}C atoms of the C8 chains (5/TPD moiety), as opposed to those of the EH groups (2/BDT moiety). This is evident from comparison with the 2D $^{13}\text{C}\{^1\text{H}\}$ HETCOR spectrum (Supporting information) for the 8 wt% C14/EH in PC₆₁BM blend, in which significantly greater intensity is observed in the correlated signals at 31 ppm in the ^{13}C dimension and at 2-3 ppm in the ^1H dimension. This is consistent with the greater population of interior ^{13}C atoms of the linear C14 chains (22/BDT moiety) relative to the δ -type carbon atoms in the branched EH alkyl groups (1/TPD moiety) and also compared to the EH/C8 blend. Moreover, the association of the ^{13}C signals at 31 ppm with linear alkyl moieties is also evidenced by the different relative intensities of the weaker correlated signals at 14 ppm (^{13}C) and 2-3 ppm (^1H), which are consistent with the comparable populations of moieties μ , *h*, and *n* in the two blends (Supporting Information Figure S13). These results collectively indicate that, in both blend materials, the PC₆₁BM functional groups interact to greater extents with the linear C8 or C14 alkyl chains of the polymers, compared to

1 the branched EH alkyl groups. As the polymer alkyl chains
2 are covalently bonded to either the TPD or BDT moieties of
3 the polymer backbone, the strong intensity correlations be-
4 tween the linear alkyl chains and PC₆₁BM functional groups
5 suggest that PC₆₁BM species are in closer proximity to moi-
6 eties of the polymer backbone that have linear alkyl chains, as
7 opposed to those with branched EH groups. The 2D NMR
8 analyses thus establish close (<1 nm) proximities of the
9 PC₆₁BM molecules with the polymer backbone and the linear
10 alkyl chains, which provide evidence of preferential interac-
11 tions of the PC₆₁BM species and the TPD acceptor moieties in
12 the EH/C8 blend, as depicted in the schematic diagram of
13 Fig. 6b.

14 Overall, the collective data presented here demonstrate
15 that PBDTTPD derivatives perform better in OPV devices
16 when the fullerene is closer to the electron accepting TPD
17 moiety. One explanation of why this polymer:fullerene ar-
18 rangement is beneficial is that the resulting intermolecular
19 interactions create a favorable energy landscape, either the
20 result of a partial charge transfer, dipole-induced dipole, or
21 quadrupolar interactions. Theoretically it has been shown
22 that the interface dipole, as well as the energetics of mole-
23 cules near the interface, can vary by hundreds of meV de-
24 pending on the donor:fullerene arrangement.^{4,18,19,21,79,80} Vari-
25 ations in energy levels, combined with how charges are sta-
26 bilized or destabilized by induced dipoles and quadrupolar
27 interactions, can lead to near zero electron-hole binding
28 energies with certain interfacial molecular
29 arrangements.^{16,18,19} These energetic shifts arising from in-
30 termolecular interactions may be a key factor in providing an
31 energetic driving force for charges to move away from the
32 polymer:fullerene interface, or out of the mixed phase in a 3-
33 phase BHJ system.^{57,62,63} Another potential explanation is
34 that the wavefunction overlap leads to high rates of charge
35 transfer and low rates of charge recombination when the
36 fullerene is in closer proximity to the acceptor unit. Both
37 lower rates of charge recombination and interfacial energetic
38 offsets have been shown with Monte Carlo simulations to
39 increase the probability of charge separation,^{81,82} and it is
40 indeed possible that either or both of these factors may ex-
41 plain the performance trend observed for the PBDTTPD de-
42 rivatives. Yet another potential explanation is that when the
43 fullerene docks with a specific part of the polymer, either
44 donor or acceptor moiety, the energetic disorder in both the
45 polymer and fullerene sites are reduced. Decreased energetic
46 disorder should increase the probability of charge separation,
47 as the local charge-carrier mobilities will remain high and
48 there will not be energetic barriers between lower and higher
49 energy sites. In this explanation of a specific intermolecular
50 arrangement leading to decreased energetic disorder, which
51 results in an improved probability for charge separation, it
52 may not be as critical as to what the arrangement is as long
53 as it is consistent. These potential explanations highlight the
54 need for further theoretical and experimental studies to
55 bring about a better molecular level understanding of the
56 variables influencing charge separation and OPV perfor-
57 mance.

58 CONCLUSION

59 It remains difficult to fully design OPV materials, in part
60 because some of the molecular factors influencing charge
separation are not yet known. The literature and work pre-
sented here suggests that a preferred intermolecular ar-
rangement exists in high-performing OPV polymer:fullerene
systems, where the fullerene is generally docked with the
electron accepting moiety of the polymer. Identification of
this trend helps to establish why certain alkyl substitution
patterns have led to successful polymers and will aid in the
more directed design of future materials. For example, new
materials should likely be designed with the electron accept-
ing moiety of the polymer being more sterically accessible
and the electron donating moiety more sterically hindered,
and/or acceptor moieties that interact favorably with the
fullerene should be identified and utilized. Observation of
this trend paves the way for further theoretical and experi-
mental studies, including determination of the intermolecu-
lar energy landscape, how this energetic landscape effects
charge separation, what intermolecular interactions lead to a
favorable energy landscape, and how factors such as interfacial
energetic disorder influence charge separation. Deter-
mination of these factors will prove critical in guiding the
design of future high-efficiency OPV material systems.

ASSOCIATED CONTENT

Supporting Information. Experimental details and proce-
dures, synthetic details, current-voltage and PV performance
characteristics, EQE data, TEM images, GIWAXS plots, 2D
¹³C{¹H} HETCOR NMR data, photoluminescence data. This
material is available free of charge via the Internet at
<http://pubs.acs.org>.

AUTHOR INFORMATION

Corresponding Authors

*mmcgehee@stanford.edu, **pierre.beaujuge@kaust.edu.sa,
***aram.amassian@kaust.edu.sa

Author Contributions

The manuscript was written through contributions of all
authors. All authors have given approval to the final version
of the manuscript.

ACKNOWLEDGMENT

This publication was supported by the Center for Advanced
Molecular Photovoltaics (Award No KUS-C1-015-21) and was
made possible by King Abdullah University of Science and
Technology (KAUST). K.R.G. and A.A. acknowledge SABIC
for a post-doctoral fellowship. G.O.N.N., K.R.G., M.D.M.,
and A.A. acknowledge the Office of Competitive Research
Funds for a GRP-CF award. T.H. gratefully acknowledges a
"DAAD Doktorandenstipendium" and the SFB
953 "Synthetic Carbon Allotropes". Use of the Stanford Syn-
chrotron Radiation Lightsource, SLAC National Accelerator
Laboratory, is supported by the U.S. Department of Energy,
Office of Science, Office of Basic Energy Sciences under Con-
tract No. DE-AC02-76SF00515. The NMR experiments were
conducted in the Central Facilities of the UCSB Materials
Research Laboratory supported by the MRSEC program of
the U.S. NSF under award no. DMR-1121053. The work at
UCSB was supported by the USARO through the Institute for

Collaborative Biotechnologies under contract no. W911NF-09-D-0001. The authors also thank Dr. Chad Risko and Prof. Jean-Luc Brédas for helpful discussions.

REFERENCES

- (1) Dou, L.; You, J.; Hong, Z.; Xu, Z.; Li, G.; Street, R. A.; Yang, Y. *Adv. Mater.* **2013**, *25*, 6642.
- (2) Darling, S. B.; You, F. *RSC Adv.* **2013**, *3*, 17633.
- (3) Angmo, D.; Gevorgyan, S. A.; Larsen-Olsen, T. T.; Søndergaard, R. R.; Hösel, M.; Jørgensen, M.; Gupta, R.; Kulkarni, G. U.; Krebs, F. C. *Org. Electron.* **2013**, *14*, 984.
- (4) Beljonne, D.; Cornil, J.; Muccioli, L.; Zannoni, C.; Brédas, J.-L.; Castet, F. *Chem. Mater.* **2011**, *23*, 591.
- (5) Jørgensen, M.; Carlé, J. E.; Søndergaard, R. R.; Lauritzen, M.; Dagnæs-Hansen, N. a.; Byskov, S. L.; Andersen, T. R.; Larsen-Olsen, T. T.; Böttiger, A. P. L.; Andreasen, B.; Fu, L.; Zuo, L.; Liu, Y.; Bundgaard, E.; Zhan, X.; Chen, H.; Krebs, F. C. *Sol. Energy Mater. Sol. Cells* **2013**, *119*, 84.
- (6) Zhou, H.; Yang, L.; You, W. *Macromolecules* **2012**, *45*, 607.
- (7) Beaujuge, P. M.; Fréchet, J. M. J. *J. Am. Chem. Soc.* **2011**, *133*, 20009.
- (8) Mishra, A.; Bäuerle, P. *Angew. Chem. Int. Ed. Engl.* **2012**, *51*, 2020.
- (9) Guo, X.; Zhou, N.; Lou, S. J.; Hennek, J. W.; Ponce Ortiz, R.; Butler, M. R.; Boudreault, P.-L. T.; Strzalka, J.; Morin, P.-O.; Leclerc, M.; López Navarrete, J. T.; Ratner, M. A.; Chen, L. X.; Chang, R. P. H.; Facchetti, A.; Marks, T. J. *J. Am. Chem. Soc.* **2012**, *134*, 18427.
- (10) Li, Y.; Zou, J.; Yip, H.; Li, C.; Zhang, Y.; Chueh, C.; Intemann, J.; Xu, Y.; Liang, P.; Chen, Y.; Jen, A. K.-Y. *Macromolecules* **2013**, *46*, 5497.
- (11) Carsten, B.; Szarko, J. M.; Son, H. J.; Wang, W.; Lu, L.; He, F.; Rolczynski, B. S.; Lou, S. J.; Chen, L. X.; Yu, L. *J. Am. Chem. Soc.* **2011**, *133*, 20468.
- (12) Carsten, B.; Szarko, J. M.; Lu, L.; Son, H. J.; He, F.; Botros, Y. Y.; Chen, L. X.; Yu, L. *Macromolecules* **2012**, *45*, 6390.
- (13) Hong, Y.-R.; Wong, H.-K.; Moh, L. C. H.; Tan, H.-S.; Chen, Z.-K. *Chem. Commun.* **2011**, *47*, 4920.
- (14) Wang, B.; Zhang, J.; Tam, H. L.; Wu, B.; Zhang, W.; Chan, M. S.; Pan, F.; Yu, G.; Zhu, F.; Wong, M. S. *Polym. Chem.* **2013**, *5*, 836.
- (15) Yi, Y.; Coropceanu, V.; Brédas, J.-L. *J. Am. Chem. Soc.* **2009**, *131*, 15777.
- (16) Verlaak, S.; Beljonne, D.; Cheyng, D.; Rolin, C.; Linares, M.; Castet, F.; Cornil, J.; Heremans, P. *Adv. Funct. Mater.* **2009**, *19*, 3809.
- (17) Yost, S. R.; Wang, L.-P.; Van Voorhis, T. *J. Phys. Chem. C* **2011**, *115*, 14431.
- (18) Linares, M.; Beljonne, D.; Cornil, J.; Lancaster, K.; Brédas, J.-L.; Verlaak, S.; Mityashin, A.; Heremans, P.; Fuchs, A.; Lennartz, C.; Idé, J.; Méreau, R.; Aurel, P.; Ducasse, L.; Castet, F. *J. Phys. Chem. C* **2010**, *114*, 3215.
- (19) Idé, J.; Mothy, S.; Savoyant, A.; Fritsch, A.; Aurel, P.; Méreau, R.; Ducasse, L.; Cornil, J.; Beljonne, D.; Castet, F. *Int. J. Quantum Chem.* **2013**, *113*, 580.
- (20) Chen, W.; Qi, D.-C.; Huang, H.; Gao, X.; Wee, A. T. S. *Adv. Funct. Mater.* **2011**, *21*, 410.
- (21) Heimel, G.; Salzmann, I.; Duhm, S.; Koch, N. *Chem. Mater.* **2011**, *23*, 359.
- (22) Rand, B. P.; Cheyng, D.; Vasseur, K.; Giebink, N. C.; Mothy, S.; Yi, Y.; Coropceanu, V.; Beljonne, D.; Cornil, J.; Brédas, J.-L.; Genoe, J. *Adv. Funct. Mater.* **2012**, *22*, 2987.
- (23) Risko, C.; McGehee, M. D.; Brédas, J.-L. *Chem. Sci.* **2011**, *2*, 1200.
- (24) Zhou, Q.; Hou, Q.; Zheng, L.; Deng, X.; Yu, G.; Cao, Y. *Appl. Phys. Lett.* **2004**, *84*, 1653.
- (25) Beaujuge, P. M.; Amb, C. M.; Reynolds, J. R. *Acc. Chem. Res.* **2010**, *43*, 1396.
- (26) Ellinger, S.; Graham, K. R.; Shi, P.; Farley, R. T.; Steckler, T. T.; Brookins, R. N.; Taranekar, P.; Mei, J.; Padilha, L. A.; Ensley, T. R.; Hu, H.; Webster, S.; Hagan, D. J.; Stryland, E. W. Van; Schanze, K. S.; Reynolds, J. R. *Chem. Mater.* **2011**, *23*, 3805.
- (27) He, Z.; Zhong, C.; Su, S.; Xu, M.; Wu, H.; Cao, Y. *Nat. Photonics* **2012**, *6*, 593.
- (28) Son, H. J.; Lu, L.; Chen, W.; Xu, T.; Zheng, T.; Carsten, B.; Strzalka, J.; Darling, S. B.; Chen, L. X.; Yu, L. *Adv. Mater.* **2013**, *25*, 838.
- (29) Zhou, H.; Yang, L.; Stuart, A. C.; Price, S. C.; Liu, S.; You, W. *Angew. Chem. Int. Ed.* **2011**, *50*, 2995.
- (30) Price, S. C.; Stuart, A. C.; Yang, L.; Zhou, H.; You, W. *J. Am. Chem. Soc.* **2011**, *133*, 4625.
- (31) Zhang, Y.; Zhou, H.; Seifert, J.; Ying, L.; Mikhailovsky, A.; Heeger, A. J.; Bazan, G. C.; Nguyen, T.-Q. *Adv. Mater.* **2013**, *25*, 7038.
- (32) Osaka, I.; Kakara, T.; Takemura, N.; Koganezawa, T.; Takimiya, K. *J. Am. Chem. Soc.* **2013**, *135*, 8834.
- (33) Xu, Y.-X.; Chueh, C.-C.; Yip, H.-L.; Ding, F.-Z.; Li, Y.-X.; Li, C.-Z.; Li, X.; Chen, W.-C.; Jen, A. K.-Y. *Adv. Mater.* **2012**, *24*, 6356.
- (34) Guo, X.; Zhang, M.; Tan, J.; Zhang, S.; Huo, L.; Hu, W.; Li, Y.; Hou, J. *Adv. Mater.* **2012**, *24*, 6536.
- (35) Dou, L.; Chen, C.; Yoshimura, K.; Ohya, K.; Chang, W.-H.; Gao, J.; Liu, Y.; Richard, E.; Yang, Y. *Macromolecules* **2013**, *46*, 3384.
- (36) Hendriks, K. H.; Heintges, G. H. L.; Gevaerts, V. S.; Wien, M. M.; Janssen, R. A. J. *Angew. Chem. Int. Ed.* **2013**, *52*, 8341.
- (37) Cabanetos, C.; El Labban, A.; Bartelt, J. A.; Douglas, J. D.; Mateker, W. R.; Fréchet, J. M. J.; McGehee, M. D.; Beaujuge, P. M. *J. Am. Chem. Soc.* **2013**, *135*, 4656.
- (38) Small, C. E.; Chen, S.; Subbiah, J.; Amb, C. M.; Tsang, S.; Lai, T.; Reynolds, J. R.; So, F. *Nat. Photonics* **2011**, *6*, 115.
- (39) Guo, X.; Zhou, N.; Lou, S. J.; Smith, J.; Tice, D. B.; Hennek, J. W.; Ortiz, R. P.; Navarrete, J. T. L.; Li, S.; Strzalka, J.; Chen, L. X.; Chang, R. P. H.; Facchetti, A.; Marks, T. J. *Nat. Photonics* **2013**, *7*, 825.
- (40) Deng, Y.; Liu, J.; Wang, J.; Liu, L.; Li, W.; Tian, H.; Zhang, X.; Xie, Z.; Geng, Y.; Wang, F. *Adv. Mater.* **2014**, *26*, 471.
- (41) Niklas, J.; Mardis, K. L.; Banks, B. P.; Grooms, G. M.; Sperlich, A.; Beaupre, S.; Dyakonov, V.; Beaupré, S.; Leclerc, M.; Xu, T.; Yu, L.; Poluektov, O. G. *Phys. Chem. Chem. Phys.* **2013**, *15*, 9562.
- (42) Alfè, M.; Apicella, B.; Barbella, R.; Bruno, A.; Ciajolo, A. *Chem. Phys. Lett.* **2005**, *405*, 193.
- (43) Aksenov, V. L.; Tropin, T. V.; Kyzyma, O. A.; Avdeev, M. V.; Korobov, M. V.; Rosta, L. *Phys. Solid State* **2010**, *52*, 1059.
- (44) Yiu, A. T.; Beaujuge, P. M.; Lee, O. P.; Woo, C. H.; Toney, M. F.; Fréchet, J. M. J. *J. Am. Chem. Soc.* **2012**, *134*, 2180.
- (45) Woo, C. H.; Beaujuge, P. M.; Holcombe, T. W.; Lee, O. P.; Fréchet, J. M. J. *J. Am. Chem. Soc.* **2010**, *132*, 15547.
- (46) Subramaniyan, S.; Xin, H.; Kim, F. S.; Shoaee, S.; Durrant, J. R.; Jenekhe, S. A. *Adv. Energy Mater.* **2011**, *1*, 854.
- (47) Guo, X.; Xin, H.; Kim, F. S.; Liyanage, A. D. T.; Jenekhe, S. A.; Watson, M. D. *Macromolecules* **2011**, *44*, 269.

- (48) Szarko, J. M.; Guo, J.; Liang, Y.; Lee, B.; Rolczynski, B. S.; Strzalka, J.; Xu, T.; Loser, S.; Marks, T. J.; Yu, L.; Chen, L. X. *Adv. Mater.* **2010**, *22*, 5468.
- (49) Liang, Y.; Feng, D.; Wu, Y.; Tsai, S.-T.; Li, G.; Ray, C.; Yu, L. *J. Am. Chem. Soc.* **2009**, *131*, 7792.
- (50) Li, Z.; Tsang, S.-W.; Du, X.; Scoles, L.; Robertson, G.; Zhang, Y.; Toll, F.; Tao, Y.; Lu, J.; Ding, J. *Adv. Funct. Mater.* **2011**, *21*, 3331.
- (51) Meager, I.; Ashraf, R. S.; Mollinger, S.; Schroeder, B. C.; Bronstein, H.; Beatrup, D.; Vezie, M. S.; Kirchartz, T.; Salleo, A.; Nelson, J.; McCulloch, I. *J. Am. Chem. Soc.* **2013**, *135*, 11537.
- (52) Li, Z.; Zhang, Y.; Tsang, S.-W.; Du, X.; Zhou, J.; Tao, Y.; Ding, J. *J. Phys. Chem. C* **2011**, *115*, 18002.
- (53) Wang, E.; Hou, L.; Wang, Z.; Ma, Z.; Hellstr, S.; Zhuang, W.; Zhang, F.; Ingan, O.; Andersson, M. R. *Macromolecules* **2011**, *44*, 2067.
- (54) Yang, L.; Zhou, H.; You, W. *J. Phys. Chem. C* **2010**, *114*, 16793.
- (55) Guo, X.; Zhou, N.; Lou, S. J.; Hennek, J. W.; Ponce Ortiz, R.; Butler, M. R.; Boudreault, P.-L. T.; Strzalka, J.; Morin, P.-O.; Leclerc, M.; López Navarrete, J. T.; Ratner, M. A.; Chen, L. X.; Chang, R. P. H.; Facchetti, A.; Marks, T. J. *J. Am. Chem. Soc.* **2012**, *134*, 18427.
- (56) Jiang, J.-M. J.; Lin, H.-K. H.; Lin, Y.-C. Y.; Chen, H. H.-C.; Lan, S.-C.; Chang, C.-K.; Wei, K.-H. *Macromolecules* **2014**, *47*, 70.
- (57) Bartelt, J. A.; Beiley, Z. M.; Hoke, E. T.; Mateker, W. R.; Douglas, J. D.; Collins, B. A.; Tumbleston, J. R.; Graham, K. R.; Amassian, A.; Ade, H.; Fréchet, J. M. J.; Toney, M. F.; McGehee, M. D. *Adv. Energy Mater.* **2013**, *3*, 364.
- (58) Zou, Y.; Najari, A.; Berrouard, P.; Beaupré, S.; Aïch, B. R.; Tao, Y.; Leclerc, M. *J. Am. Chem. Soc.* **2010**, *132*, 5330.
- (59) Piliago, C.; Holcombe, T. W.; Douglas, J. D.; Woo, C. H.; Beaujuge, P. M.; Fréchet, J. M. J. *J. Am. Chem. Soc.* **2010**, *132*, 7595.
- (60) Zhang, Y.; Hau, S. K.; Yip, H.-L.; Sun, Y.; Acton, O.; Jen, A. K.-Y. *Chem. Mater.* **2010**, *22*, 2696.
- (61) Bartelt, J. A.; Douglas, J. D.; Mateker, W. R.; Labban, A. E.; Tassone, C. J.; Toney, M. F.; Fréchet, J. M. J.; Beaujuge, P. M.; McGehee, M. D. *Adv. Energy Mater.* **Early View**, DOI: 10.1002/aenm.201301733.
- (62) Shoaee, S.; Subramanian, S.; Xin, H.; Keiderling, C.; Tuladhar, P. S.; Jamieson, F.; Jenekhe, S. A.; Durrant, J. R. *Adv. Funct. Mater.* **2013**, *23*, 3286.
- (63) Westacott, P.; Tumbleston, J. R.; Shoaee, S.; Fearn, S.; Bannock, J. H.; Gilchrist, J. B.; Heutz, S.; deMello, J.; Heeney, M.; Ade, H.; Durrant, J.; McPhail, D. S.; Stingelin, N. *Energy Environ. Sci.* **2013**, *6*, 2756.
- (64) Amb, C. M.; Chen, S.; Graham, K. R.; Subbiah, J.; Small, C. E.; So, F.; Reynolds, J. R. *J. Am. Chem. Soc.* **2011**, *133*, 10062.
- (65) Treat, N. D.; Varotto, A.; Takacs, C. J.; Batara, N.; Al-Hashimi, M.; Heeney, M. J.; Heeger, A. J.; Wudl, F.; Hawker, C. J.; Chabinc, M. L. *J. Am. Chem. Soc.* **2012**, *134*, 15869.
- (66) Chu, C.-W.; Shrotriya, V.; Li, G.; Yang, Y. *Appl. Phys. Lett.* **2006**, *88*, 153504.
- (67) Yang, B.; Guo, F.; Yuan, Y.; Xiao, Z.; Lu, Y.; Dong, Q.; Huang, J. *Adv. Mater.* **2013**, *25*, 572.
- (68) Shuttle, C. G.; O'Regan, B.; Ballantyne, A. M.; Nelson, J.; Bradley, D. D. C.; de Mello, J.; Durrant, J. R. *Appl. Phys. Lett.* **2008**, *92*, 093311.
- (69) Vandewal, K.; Tvingstedt, K.; Gadisa, A.; Inganäs, O.; Manca, J. V. *Phys. Rev. B* **2010**, *81*, 125204.
- (70) Graham, K. R.; Erwin, P.; Nordlund, D.; Vandewal, K.; Li, R.; Ngongang Ndjawa, G. O.; Hoke, E. T.; Salleo, A.; Thompson, M. E.; McGehee, M. D.; Amassian, A. *Adv. Mater.* **2013**, *25*, 6076.
- (71) Marcus, R. A. *J. Phys. Chem.* **1990**, *94*, 4963.
- (72) Brunschwig, B. S.; Ehrenson, S.; Sutin, N. *J. Phys. Chem.* **1987**, *91*, 4714.
- (73) Hou, Y.; Bardo, A. M.; Martinez, C.; Higgins, D. A. *J. Phys. Chem. B* **2000**, *104*, 212.
- (74) Rhodes, T. A.; Farid, S.; Goodman, J. L.; Gould, I. R.; Young, R. H. *J. Am. Chem. Soc.* **1999**, *121*, 5340.
- (75) Ojala, A.; Petersen, A.; Fuchs, A.; Lovrincic, R.; Pölking, C.; Trollmann, J.; Hwang, J.; Lennartz, C.; Reichelt, H.; Höffken, H. W.; Pucci, A.; Erk, P.; Kirchartz, T.; Würthner, F. *Adv. Funct. Mater.* **2012**, *22*, 86.
- (76) Miller, N. C.; Cho, E.; Junk, M. J. N.; Gysel, R.; Risko, C.; Kim, D.; Sweetnam, S.; Miller, C. E.; Richter, L. J.; Kline, R. J.; Heeney, M.; McCulloch, I.; Amassian, A.; Acevedo-Feliz, D.; Knox, C.; Hansen, M. R.; Dudenko, D.; Chmelka, B. F.; Toney, M. F.; Brédas, J.-L.; McGehee, M. D. *Adv. Mater.* **2012**, *24*, 6071.
- (77) Ko, S.; Hoke, E. T.; Pandey, L.; Hong, S.; Mondal, R.; Risko, C.; Yi, Y.; Noriega, R.; McGehee, M. D.; Brédas, J.-L.; Salleo, A.; Bao, Z. *J. Am. Chem. Soc.* **2012**, *134*, 5222.
- (78) Piersimoni, F.; Chambon, S.; Vandewal, K.; Mens, R.; Boonen, T.; Gadisa, A.; Izquierdo, M.; Filippone, S.; Ruttens, B.; D'Haen, J.; Martin, N.; Lutsen, L.; Vanderzande, D.; Adriaensens, P.; Manca, J. V. *J. Phys. Chem. C* **2011**, *115*, 10873.
- (79) Mothy, S.; Guillaume, M.; Idé, J.; Castet, F.; Ducasse, L.; Cornil, J.; Beljonne, D. *J. Phys. Chem. Lett.* **2012**, *3*, 2374.
- (80) D'Avino, G.; Mothy, S.; Muccioli, L.; Zannoni, C.; Wang, L.; Cornil, J.; Beljonne, D.; Castet, F. *J. Phys. Chem. C* **2013**, *117*, 12981.
- (81) Burke, T. M.; McGehee, M. D. *Adv. Mater.* **2014**, *26*, 1923.
- (82) Groves, C. *Energy Environ. Sci.* **2013**, *6*, 1546.

